









A proteomic atlas of the neointima identifies novel druggable targets for preventive therapy

Michael Wierer ^{1†}, Julia Werner ^{2†}, Jana Wobst ^{2,3†}, Adnan Kastrati ^{2,3},
Ganildo Cepele ², Redouane Aherrahrou ⁴, Hendrik B. Sager ^{2,3},
Jeanette Erdmann ^{5,6}, Martin Dichgans⁷, Veit Flockerzi⁸, Mete Civelek ⁴,
Alexander Dietrich ⁹, Matthias Mann^{1*‡}, Heribert Schunkert^{2,3‡}, and
Thorsten Kessler ^{2,3*‡}

¹Department of Proteomics and Signal Transduction, Max-Planck Institute of Biochemistry, Planegg, Germany ²Department of Cardiology, German Heart Centre Munich, Technical University of Munich, Munich, Germany ³German Centre for Cardiovascular Research (DZHK e. V.), partner site Munich Heart Alliance, Munich, Germany ⁴Department of Biomedical Engineering, Center for Public Health Genomics, University of Virginia, Charlottesville, VA, USA ⁵Institute for Cardiogenetics, University of Lübeck, Lübeck, Germany ⁶German Centre for Cardiovascular Research (DZHK e. V.), partner site Hamburg/Kiel/Lübeck, Lübeck, Germany ⁷Institute for Stroke and Dementia Research, University Hospital, Ludwig-Maximilians-University, Munich, Germany ⁸Experimental and Clinical Pharmacology and Toxicology, Saarland University, Homburg, Germany; and ⁹Walther-Straub-Institute of Pharmacology and Toxicology, Member of the Center for Lung Research (DZL), Ludwig-Maximilians-University, Munich, Germany

Received 21 July 2020; revised 30 November 2020; editorial decision 19 February 2021; accepted 19 February 2021; online publish-ahead-of-print 8 April 2021

See page 1786 for the editorial comment on this article (doi: 10.1093/eurheartj/ehab144)

Aims

In-stent restenosis is a complication after coronary stenting associated with morbidity and mortality. Here, we sought to investigate the molecular processes underlying neointima formation and to identify new treatment and prevention targets.

Methods and results

Neointima formation was induced by wire injury in mouse femoral arteries. High-accuracy proteomic measurement of single femoral arteries to a depth of about 5000 proteins revealed massive proteome remodelling, with more than half of all proteins exhibiting expression differences between injured and non-injured vessels. We observed major changes in the composition of the extracellular matrix and cell migration processes. Among the latter, we identified the classical transient receptor potential channel 6 (TRPC6) to drive neointima formation. While *Trpc6*^{-/-} mice presented reduced neointima formation compared to wild-type mice (1.44 ± 0.39 vs. 2.16 ± 0.48, *P* = 0.01), activating or repressing TRPC6 in human vascular smooth muscle cells resulted in increased [vehicle 156.9 ± 15.8 vs. 1-oleoyl-2-acetyl-sn-glycerol 179.1 ± 8.07 (10³ pixels), *P* = 0.01] or decreased migratory capacity [vehicle 130.0 ± 26.1 vs. SAR7334 111.4 ± 38.0 (10³ pixels), *P* = 0.04], respectively. In a cohort of individuals with angiographic follow-up (*n* = 3068, males: 69.9%, age: 59 ± 11 years, follow-up 217.1 ± 156.4 days), homozygous carriers of a common genetic variant associated with elevated *TRPC6* expression were at increased risk of restenosis after coronary stenting (adjusted odds ratio 1.49, 95% confidence interval 1.08–2.05; *P* = 0.01).

Conclusions

Our study provides a proteomic atlas of the healthy and injured arterial wall that can be used to define novel factors for therapeutic targeting. We present TRPC6 as an actionable target to prevent neointima formation secondary to vascular injury and stent implantation.

* Corresponding authors. Tel: +49 89 1218 2786, Fax: +49 89 1218 4013, Email: thorsten.kessler@tum.de (T.K.); Tel: +49 89 8578 2558, Fax: +49 89 8578 2412, Email: mmann@biochem.mpg.de (M.M.)

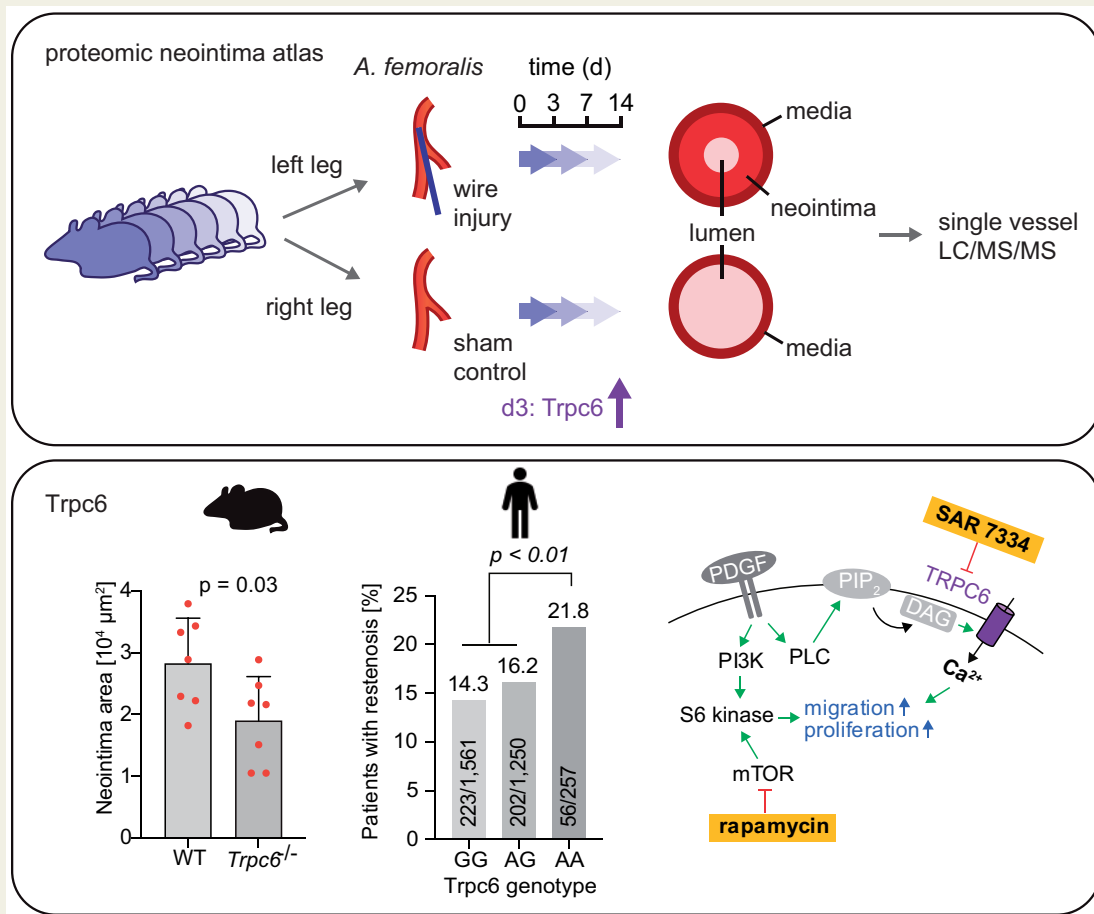
[†]These first three authors contributed equally to the study.

[‡]These authors provided equal supervision of this work.

© The Author(s) 2021. Published by Oxford University Press on behalf of the European Society of Cardiology.

This is an Open Access article distributed under the terms of the Creative Commons Attribution Non-Commercial License (<http://creativecommons.org/licenses/by-nc/4.0/>), which permits non-commercial re-use, distribution, and reproduction in any medium, provided the original work is properly cited. For commercial re-use, please contact journals.permissions@oup.com

Graphical Abstract



Study scheme and hypothesis: TRPC6 inhibition provides a complementary strategy for inhibition of neointima formation by blocking migration and proliferation of smooth muscle cells. DAG, diacylglycerol; ER, endoplasmic reticulum; IP₃(-R), inositol trisphosphate (receptor); LC, liquid chromatography; MS, mass spectrometry; PDGF, platelet-derived growth factor; mTOR, mammalian target of rapamycin; PIP₂, phosphatidylinositol-4, 5-bisphosphate; PI3K, phosphoinositide 3-kinase; PLC, phospholipase C.

Keywords

Proteomics • Restenosis • Vascular remodelling • Genetics

Translational perspective

In-stent restenosis is a complication after coronary stenting associated with morbidity and mortality. Using high-accuracy proteomic measurement of single femoral arteries in mice after wire-induced injury, we identified the classical transient receptor potential channel 6 (TRPC6) as a protein driving neointima formation. Inhibiting TRPC6 might be a promising strategy to prevent neointima formation secondary to vascular injury and stent implantation.

Introduction

Cardiovascular diseases, in particular atherosclerosis of coronary, carotid, or peripheral arteries, are the leading cause of death worldwide.¹ Restoration of blood flow often requires interventional

treatment including balloon angioplasty and stenting of coronary, carotid, or peripheral arteries.² Such procedures frequently lead to formation of sub-endothelial scars, known as neointima.³ Neointima formation can become a critical disease itself, when it massively reduces blood flow in the context of restenosis. Depending on the

underlying pathology, location and type of intervention, the incidence of restenosis ranges between 6% and 40%, which thereby becomes the most relevant limitation of interventional treatment of atherosclerotic lesions. Importantly, restenosis also influences prognosis: in comparison to patients not suffering from restenosis, patients with restenosis display a higher mortality.⁴ Better therapeutic strategies to prevent neointima formation are therefore of major clinical importance.

While the proteome of atherosclerosis has been studied before,^{5–8} there are few proteomic studies of vascular injury^{9,10} and no unbiased analysis following acute injury to mature neointima formation. To detect key drivers of vascular remodelling and to develop new strategies for prevention and therapy of restenosis, we here set out to study time-resolved proteomic changes in single femoral arteries following vascular injury.

Methods

Wire-induced femoral artery injury

All animal studies were performed with permission of the government of Upper Bavaria (55.2-1-54-2532-17-14) and according to international guidelines. *Trpc6*^{-/-} mice have been described previously.¹¹ Wire injury was performed in eight to 12 weeks old C57BL/6J (Jackson Laboratories, Bar Harbor, ME, USA), and *Trpc6*^{-/-} as well as wild-type mice from the same colony on a C57BL/6J background as described previously.¹² Details are available in the [Supplementary material online](#).

Histology and morphometry

Femoral arteries were embedded in paraffin. Two-micrometre serial cross-sections were cut starting from the ligation as reference point using a microtome (HM 340E, Thermo Fisher Scientific, Waltham, MA, USA). Sections were mounted on microscope slides, deparaffinized and rehydrated in graded alcohol. Ten to 15 sections per femoral artery at 25 μ m intervals were stained with haematoxylin and eosin and embedded in paraffin (Mediate Cancer Diagnostics, Chicago, IL, USA). Details are available in the [Supplementary material online](#).

Sample preparation for proteomic analysis

Snap-frozen femoral arteries from C57BL/6J were manually disrupted in 100 μ L lysis buffer (6 M GdmCl, 10 mM TCEP, 100 mM Tris-HCl, pH 8.5) using a micro tissue grinder (Thermo Fisher Scientific, Waltham, MA, USA). After the arteries were fully dissolved, samples were incubated for 10 min at 99°C and sonicated in a Bioruptor for 20 min at 30 s on/30 s off cycles. Details are available in the [Supplementary material online](#).

Liquid chromatography-tandem mass spectrometry analysis

Peptides were separated on a reverse phase column (50 cm length, 75 μ m inner diameter) packed in-house with ReproSil-Pur C18-AQ 1.9 μ m resin (Dr Maisch GmbH, Ammerbuch, Germany). Reverse-phase chromatography was performed with an EASY-nLC 1000 ultra-high pressure system, coupled to a Q-Exactive HF Mass Spectrometer (Thermo Fisher Scientific, Waltham, MA, USA). Details are available in the [Supplementary material online](#).

Computational mass spectrometry-data analysis

Mass spectrometry (MS) raw files were analysed by the MaxQuant software¹³ (version 1.5.3.54) and peak lists searched against the mouse Uniprot FASTA database (UP000000589_10090.fasta and UP000000589_10090_additional.fasta), and a common contaminants database (247 entries) by the Andromeda search engine. Details are available in the [Supplementary material online](#). All downstream bioinformatic analyses were performed with Perseus¹⁴ (v. 1.6.0.2078) and R (v. 3.5.3). Protein groups only identified by site false discovery rate (FDR), only from peptides identified also in the reverse database, or belonging to the potential contaminant list were excluded from the analyses. For principal component analysis, analysis of variance and Student's *t*-test, missing values were imputed with a width of 0.2 and a downshift of 1.8 over the total matrix.

Cell culture

Human aortic smooth muscle cells (SMCs) were purchased from PromoCell (Heidelberg, Germany) and cultured at 37°C in a humidified 5% CO₂ atmosphere in the recommended cell culture medium (PromoCell, Heidelberg, Germany). Details are available in the [Supplementary material online](#).

Cell migration assay

For *in vitro* scratch wound assays, cells were seeded in 24 well plates at a density of 100 000 cells per well. After they had grown to confluence for 24 h the cell monolayer was scratched in the middle with a 200 μ L pipette tip. *In vitro* wound reclosure was measured as Δt_{0-t_1} (6 h), Δt_{0-t_2} (8 h), and Δt_{0-t_3} (12 h) in pixels. Details are available in the [Supplementary material online](#).

Cell proliferation assays

Cell proliferation was assessed using of a colorimetric bromodeoxyuridine (BrdU) enzyme-linked immunosorbent assay according to manufacturer's protocol (Roche Applied Science, Penzberg, Germany) or the BrdU cell proliferation assay kit according to the manufacturer's instructions (Cell Signaling Technology, Danvers, MA, USA). Details are available in the [Supplementary material online](#).

Analysis of binary restenosis in humans

Available genotyping data from previous genome-wide association studies and subsequent analyses^{15,16} were used to correlate rs2513192 genotype and risk of binary restenosis. Rs2513192 genotype was available in 4247 individuals which were scheduled for routine follow-up angiography after 6 months and 6028 lesions. Characteristics are depicted in [Supplementary material online, Table S3](#). Information on binary restenosis, defined as a diameter reduction of 50% or more, was available in 3068 (72.2%) individuals (one or more lesions with binary restenosis) and 4279 (71%) lesions. A logistic regression model with computation of odds ratios (OR) and 95% confidence intervals (CI) was used to assess the association of rs2513192 genotype with the primary endpoint binary restenosis after adjustment for other covariates. Details are available in the [Supplementary material online](#).

Statistical analyses

Distribution of data was assessed using Kolmogorov–Smirnov test. Unless otherwise stated, normally distributed data were analysed using Student's unpaired/paired *t*-test. Not normally distributed data were analysed with Mann–Whitney test. Categorical data were analysed using χ^2 test. *P*-values <0.05 were regarded significant. GraphPad Prism version

8.0.1 for Mac OS X (GraphPad Software, La Jolla, CA, USA) was used. Details are available in the [Supplementary material online](#) together with the method used.

Results

Changes in the vascular proteome secondary to vascular injury in mice

Vascular injury results in substantial tissue remodelling of blood vessels and eventually leads to the formation of a neointima. To study this process on the proteomic level, we induced vascular injury by wirescratching of the left femoral artery of mice ($n=6$ each) and withdrew the vessels after three to 14 days ([Figure 1A](#)). We extracted and lysed both injured and non-injured arteries, digested the containing proteins to peptides and measured them by high-resolution MS. In total, we quantified 4836 proteins from three different timepoints and six biological replicates per timepoint and condition ([Supplementary material online, Table S1](#)). The reproducibility was very high indicated by a median coefficient of variation (CV) $<2\%$ for all conditions ([Figure 1B](#)). Notably, wire-scratched femoral arteries had about 700–1100 quantified proteins more than non-injured arteries at any timepoint, with averages of 4286 vs. 3349 proteins per single blood vessel ([Figure 1C](#)). Principal component analysis revealed a clear separation of non-injured and injured single arteries in the first component ([Figure 1D](#)). Together, this reflected a strong proteomic response which was very prominent already at three days after vascular injury and partly driven by the infiltration of other cell types with cell-specific protein sets ([Supplementary material online, Figure S1](#)). Analysis of variance followed by unsupervised cluster analysis over all conditions supported this. Choosing a stringent cut-off filter, 2918 proteins exhibited statistically significant changes in their expression levels (FDR <0.01 , $s_0=1$) ([Figure 1E](#)). While the majority (58%) of these were already up-regulated at Day 3 after injury (Clusters V and VI), we also observed proteins with transient (Cluster IV; 9%) or late regulation (Cluster III; 15%). In contrast, 18% of significantly changed proteins were down-regulated upon injury—all of them already at Day 3 after injury (Clusters I and II).

To better understand the processes involved in neointima formation, we next performed pairwise comparisons of injured and non-injured vessels at each timepoint and pathway analyses on significantly regulated proteins (FDR <0.01 , $s_0=1$) ([Figure 2A and B](#)). Proteins up-regulated in response to vascular injury were primarily involved in pathways related to immune response, cell adhesion, cell activation, extracellular matrix (ECM), proliferation, and migration ([Figure 2C and D, Supplementary material online, Table S2](#)). Remarkably, more than 70% of all proteins identified from the gene ontology set 'innate immune response' were robustly up-regulated at Day 7 after vascular injury ([Figure 2C](#)). Proteins relevant for coagulation, cell proliferation, and cell migration displayed most differential regulation at Day 3, indicating specific pathway activation at an early stage after injury. The most prominent regulated set was glycoproteins, representing about 26%, 18%, and 23% of all up-regulated proteins at Day 3, 7, and 14, respectively ([Figure 2D](#)). Together with the large number of extracellular proteins, this provides strong evidence for an extensive remodelling of the membrane and ECM

compartment. Interestingly, glycoproteins—in particular those involved in cell–cell contacts—were the largest subgroup of significantly down-regulated proteins upon vessel injury. This was most prominent at Day 14, where 29% of all down-regulated proteins reflected cell junction proteins.

A pathway analysis for the clusters defined in [Figure 1D](#) revealed a similar picture. Cell junction proteins were highly enriched in Cluster II (down-regulation from Day 3 on), while coagulation proteins were most strongly enriched in Cluster IV (transient up-regulation at Day 3) ([Supplementary material online, Figure S2](#)).

Effects of vascular injury on the core matrisome and matrisome-associated components in mice

To follow ECM remodelling, we selected all significantly regulated proteins that overlap with a previously defined list of core matrisome proteins.^{17,18} Of these proteins, 42% were down-regulated, which is a more than two-fold enrichment compared with all regulated proteins (compare [Figures 3A and 1E](#)). Down-regulation of ECM core proteins is therefore a specific property of tissue remodelling in response to vascular injury at a global scale.

Laminins are major components of the basal lamina and mediate important functions such as cell differentiation, migration, and adhesion.¹⁹ Strikingly, five out of the six laminins were down-regulated (Lama2, -a4, -a5, -b2, and -c1) starting at Day 3, with about two-fold down-regulation at Day 7 and constant effect sizes at Day 14 ([Figure 3A and B](#)). Only Lamb1 presented a different behaviour, with two-fold up-regulation at Day 14 ($P<0.00004$). Hence, in addition to an overall decrease of laminins in injured vessels, there is a change in the laminin subunit composition, with a four-fold increase in Lamb1 containing laminins relative to Lamb2 containing laminins in response to wire injury.

Similar to the components of the basement membrane, we also observed changes in the collagen composition of the ECM ([Figure 3A and C](#)). For instance, all collagen VI subtypes were significantly down-regulated at Day 3. While the majority remained down-regulated over the whole time course, Col6a5 and Col6a6 were up-regulated at Day 14, indicating a switch in subunit composition also for collagen VI.

Other changes of collagen expression involved a more than eight-fold down-regulation of Col19a1 at Day 7 after wire injury ($P<10^{-6}$) ([Figure 3C](#)). Although the molecular function of collagen XIX is unknown, its expression has been linked to positive regulation of muscle differentiation.²⁰ Down-regulation might therefore activate the proliferation phenotype of vascular SMCs. Col8a1 and Col14a1 were two-fold ($P<10^{-5}$) and >4 -fold ($P<0.003$) up-regulated at Day 14, respectively. While collagen VIII is known to promote neointima formation upon vessel injury,²¹ the involvement of collagen XIV in this process has not been described before.

Extracellular matrix remodelling involves the enzymatic activities of different proteases, which are under tight control of protease inhibitors.²² To understand the origin of changes in the ECM proteome in response to vascular injury, we next focused on matrisome-associated proteins that were significantly regulated in our time course ([Supplementary material online, Figure S3](#)). Collagen VI is known to be cleaved by matrix metalloproteases Mmp2 and Mmp9²³

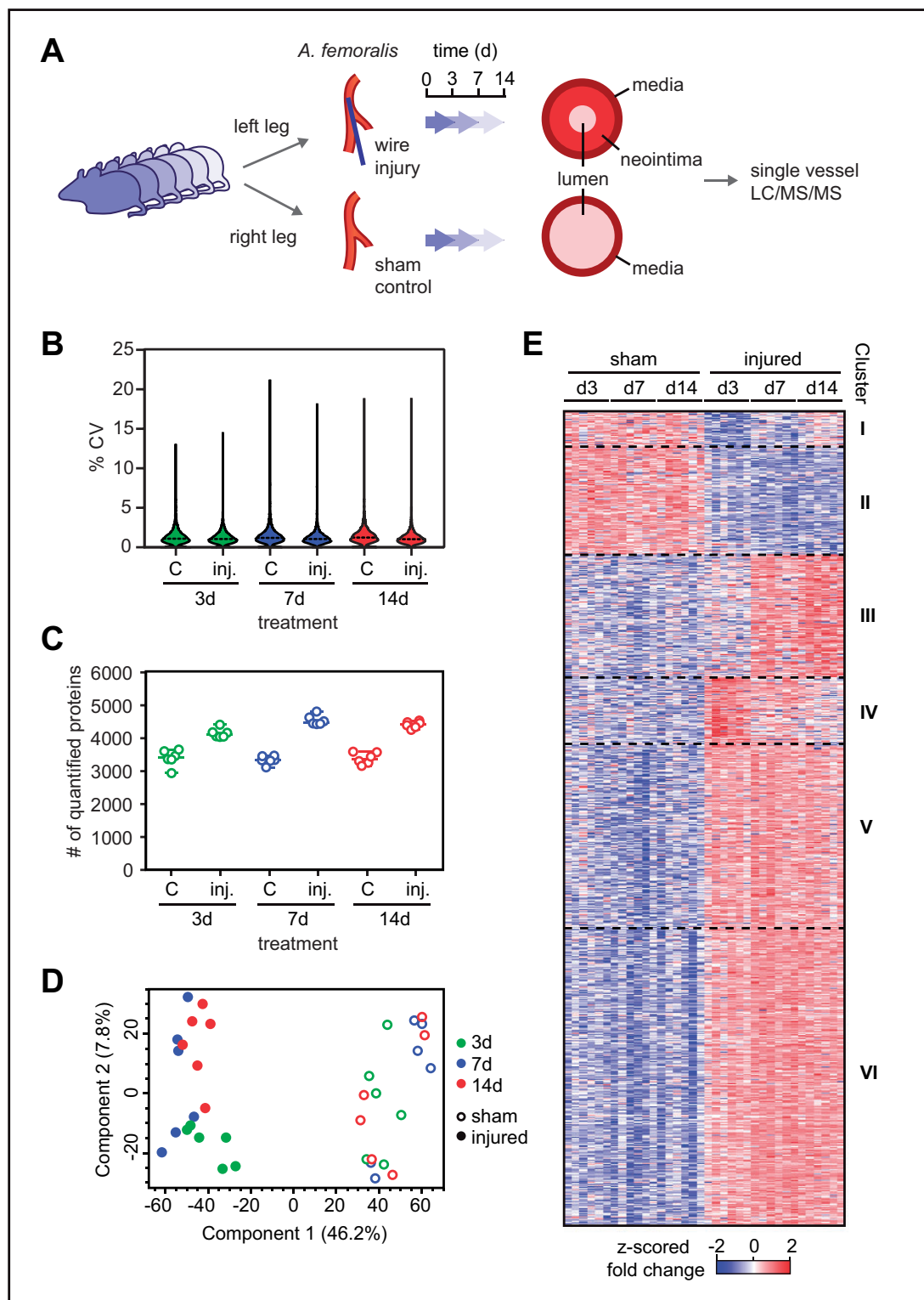


Figure 1 Deep proteomic analysis of neointima formation. (A) Schematic representation of the study design ($n = 6$ mice at each timepoint). (B) Median percentage coefficient of variation (% CV) distribution per condition and timepoint. (C) Number of quantified proteins per sample. (D) Principal component analysis of all samples. (E) Unsupervised hierarchical clustering of z-scored (LFQ) intensities of significantly regulated proteins into six protein expression clusters (analysis of variance, false discovery rate < 0.01 , $s_0 = 1$). The majority (58%) of proteins were already up-regulated at Day 3 after injury (Clusters V and VI); we further observed proteins with transient (Cluster IV; 9%) or late regulation (Cluster III; 15%). 18% of significantly changed proteins were down-regulated upon injury—all of them already at Day 3 after injury (Clusters I and II). C, control/sham; CV, coefficient of variation; d, day(s); inj, injured; LC/MS, liquid chromatography/mass spectrometry.

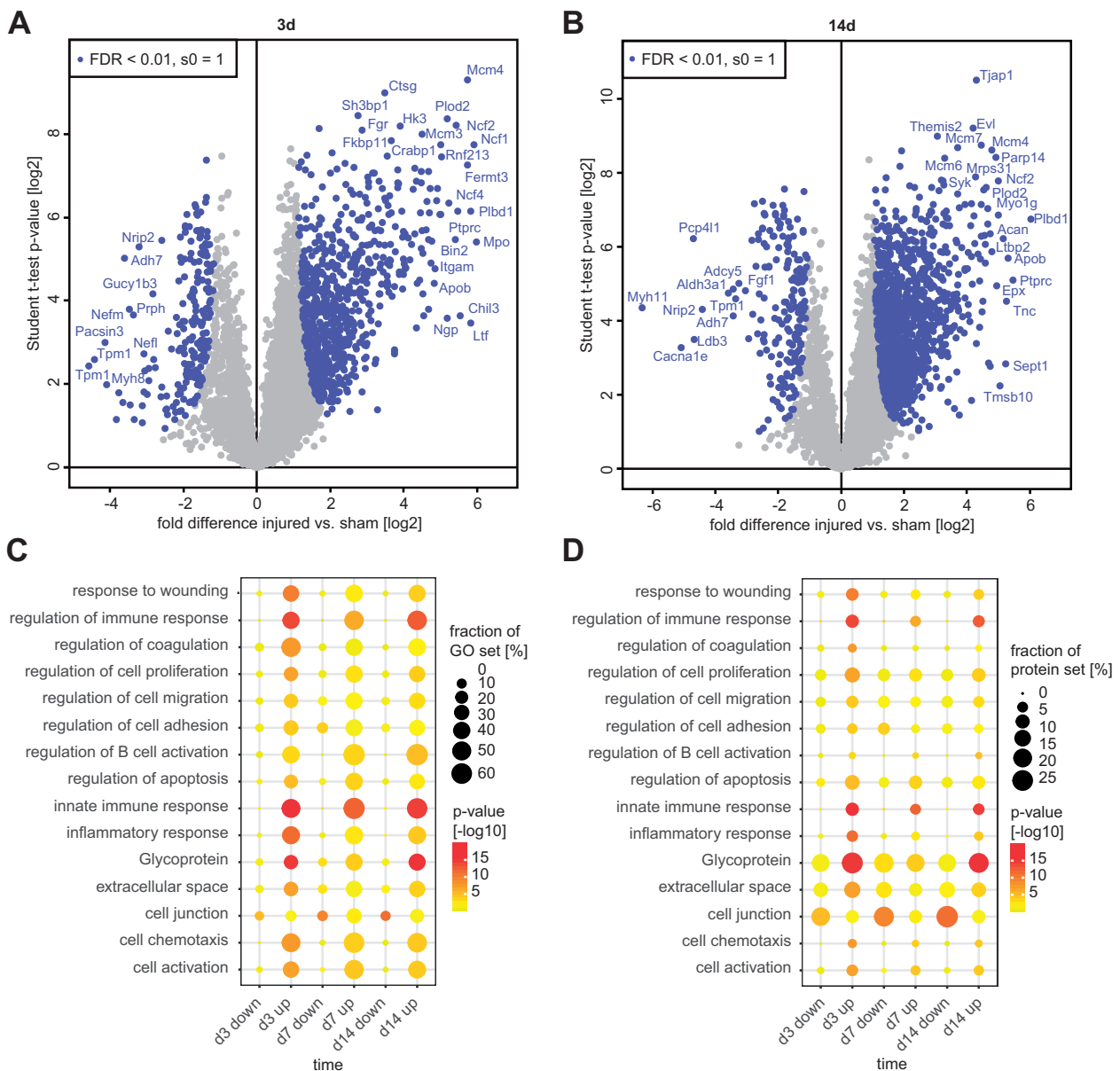


Figure 2 Pathway analysis of regulated proteins at each timepoint. (A, B) Unpaired Student's *t*-test results of injured vs. sham-treated femoral arteries at three (A) and 14 days (B) after vessel injury. Blue dots indicate significantly regulated proteins (false discovery rate < 0.01, $s_0 = 1$). (C, D) Gene Ontology (GO) term enrichment analysis (Fisher's exact test) of significantly regulated proteins. Colours of the dots correspond to the *P*-values, size represents fraction of regulated proteins of the GO set (C), or fraction of annotated proteins of regulated proteins (D). d, day(s); FDR, false discovery rate.

and in our dataset, both proteases were up-regulated in response to vascular injury, yet with different timing. While Mmp9 was most strongly up-regulated at Day 3 after injury (>16-fold, $P < 10^{-5}$), expression of Mmp2 was not altered at this timepoint and started to increase at Day 7 (Figure 3D). As the down-regulation of collagen VI was most prominent from Day 3 on, it is likely linked to an increased expression of Mmp9. Likewise, increased Mmp14 expression might be causative for the degradation of laminins as one of the main Mmp14 substrates.²⁴

Regulation of migration factors during neointima formation in mice

Migration of SMCs is a hallmark of neointima formation and we therefore focused on proteins annotated for regulatory functions in cell migration (Figure 4A and B). Comparing significantly changed proteins at Days 3 and 14 after injury, we observed a large number of migration factors to be constantly up-regulated compared with sham-treated vessels (e.g. Ptpcr, Myo1g). In contrast, we also

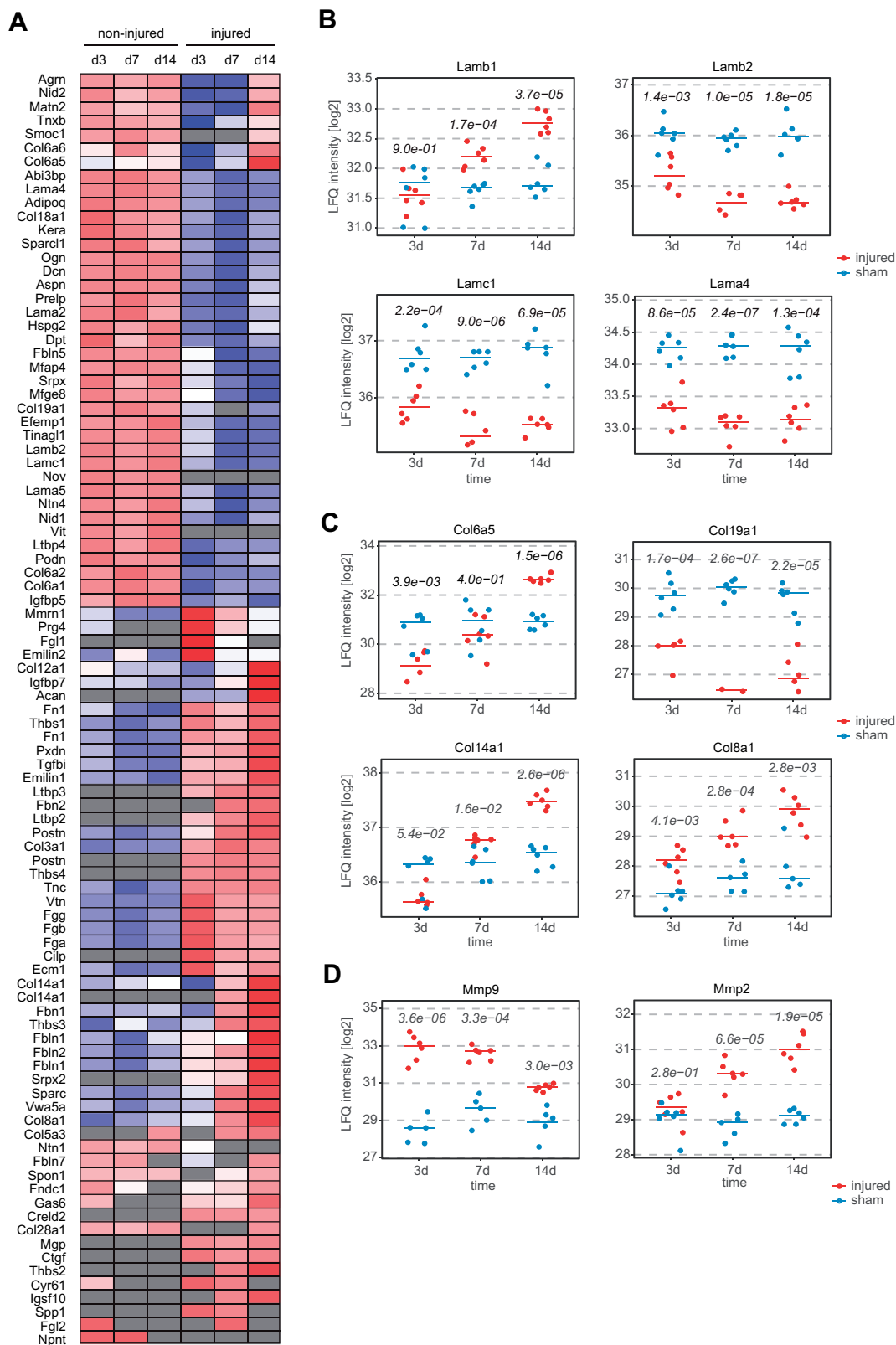


Figure 3 Time-resolved analysis of extracellular matrix remodelling upon vessel injury. **(A)** Analysis of variance significantly regulated proteins that are also annotated as core extracellular matrix proteins.^{17,18} Heatmap represents z-scored average protein intensities. **(B–D)** Protein intensities of selected core matrisomal (B, C), or matrisome-associated (D) proteins. P-values were derived from unpaired Student's *t*-test statistics. d, day(s); LFQ, label-free quantitation.

identified factors specifically up-regulated at early (e.g. Itga2b, Spp1) or late (e.g. Itga11, Fadd) timepoints (Figure 4B).

Other prominent surface markers, which altered their expression in response to injury, included Cd34, Cd44, and Cd47 (Figure 4C). Cd34 is a marker for vascular endothelial cells known for its capability to block cell adhesion processes of particularly mast cells^{25,26} and in our dataset, it is transiently down-regulated at Day 3 (four-fold, $P < 0.001$). This down-regulation in response to injury has not been reported previously, and might permit adhesion of cells. In contrast, Cd44 supports the adhesion of activated lymphocytes to endothelium and SMCs,²⁷ and accordingly was up-regulated at all timepoints. Up-regulation of Cd47 at Day 7 ($P = 0.0017$) and Day 14 ($P = 0.0004$) likely modulates proinflammatory functions, mediated by interaction with macrophage migration inhibitory factor.²⁸

Among the least expressed proteins in our study were low abundant migration factors that were specifically expressed after injury, including Itga11, Elane, and the ion channel *Trpc6*, which regulates migration of breast cancer cell lines,²⁹ transepithelial migration of leukocytes,³⁰ and chemotaxis of murine neutrophils³¹ (Figure 4D).

Trpc6 promotes neointima formation in mice

We next set out to mine our dataset for new targets that could potentially be exploited for pharmacological applications. We found a single protein that fulfilled the following five pre-specified criteria: (i) increased expression after vascular injury, (ii) transient expression with highest levels in the early phase, (iii) low expression or non-detectable in non-injured tissue, (iv) previous association with cell migration, and (v) available pharmacological inhibitor. This protein was the classical *Trpc6*, a non-selective cation channel functional in the plasma membrane of endothelial³² and arterial SMCs³³ (as well as neutrophils^{31,34}). In particular, the low abundance in healthy vessels and the up-regulation of *Trpc6* protein levels at the earliest timepoint (Figure 4D) prompted further investigation as we specifically wanted to study targets that might initiate neointima formation.

To test whether *Trpc6* is involved in neointima formation *in vivo*, we performed wire injury in *Trpc6*^{-/-} and wild-type mice ($n = 7$ each) and analysed neointima formation after 28 days (Figure 5A). *Trpc6*^{-/-} mice displayed reduced neointima area compared with wild-type mice [1.90 ± 0.71 vs. 2.82 ± 0.73 ($10^4 \mu\text{m}^2$), $P = 0.03$] (Figure 5B), whereas media area was comparable between the genotypes [1.47 ± 0.55 vs. 1.52 ± 0.31 ($10^4 \mu\text{m}^2$), $P = 0.82$] (Figure 5C). The neointima-media ratio was also significantly reduced (1.44 ± 0.39 vs. 2.16 ± 0.48 , $P = 0.01$) (Figure 5D). Collectively, these results provide evidence for a role of *Trpc6* in neointima formation in mice.

Trpc6 as a target in human vascular smooth muscle cells

To investigate the influence of *Trpc6* on SMCs, we analysed migration and proliferation of human aortic vascular SMCs *in vitro*. The TRPC6 activator 1-oleoyl-2-acetyl-sn-glycerol (OAG) led to an increase in *in vitro* wound reclosure compared with vehicle treatment after 8 and 12 h [vehicle 69.1 ± 15.71 vs. OAG 93.1 ± 8.22 (10^3 pixels), $P = 0.01$ and vehicle 156.9 ± 15.8 vs. OAG 179.1 ± 8.07 (10^3 pixels), $P = 0.01$, $n = 5$ each, respectively] (Figure 6A). OAG also enhanced proliferation of human

aortic SMCs [vehicle 0.08 ± 0.09 vs. OAG 0.31 ± 0.2 (absorbance units), $P < 0.01$, $n = 8$] (Figure 6B). On the contrary, the TRPC6 inhibitor SAR7334 reduced vascular SMC migration after 12 h [111.4 ± 38.0 vs. 130.0 ± 26.1 (10^3 pixels), $P = 0.04$, $n = 6$] (Figure 6C). In line with these results, coating of cell culture dishes with SAR7334 reduced local migration of human aortic SMC compared with control treatment [268.2 ± 105.6 vs. 359.2 ± 96.3 (10^3 pixels), $P = 0.035$, $n = 5$] (Figure 6D).

An expression single nucleotide polymorphism at the TRPC6 locus is linked to smooth muscle cell proliferation and restenosis in humans

To investigate whether genetically determined *TRPC6* expression influences SMC migration, we queried the GTEx dataset³⁵ and identified rs2513192 as a common expression single nucleotide polymorphism (eSNP) for *TRPC6* in arteries (Figure 7A and B). The rs2513192 genotype was also associated with proliferation of human aortic SMCs *in vitro* after stimulation with platelet-derived growth factor (PDGF) with the A-allele linked to enhanced SMC proliferation (Figure 7C).

To test whether genetically determined *TRPC6* expression associates with restenosis after coronary stenting, we analysed its occurrence by standardized quantitative coronary analysis in 3068 individuals and 4279 lesions undergoing coronary stenting (Figure 7D). Baseline and procedural characteristics are listed in Supplementary material online, Table S3. Restenosis, defined as a diameter reduction of more than 50%, occurred in 65 of 369 AA lesions compared with 498 of 3910 GG/AG lesions [17.6 vs. 12.7%, $P = 0.01$; OR 1.46 (95% CI 1.08–1.95), $P = 0.01$] (Figure 7E) with a significant gene-dosage effect (GG 12.5 vs. AG 13.1 vs. AA 17.6%, $P = 0.03$). In a multivariate analysis of patients that underwent coronary stenting (Supplementary material online, Table S4), the AA genotype remained a predictor of binary restenosis [OR_{adj} 1.49 (95% CI 1.08–2.05), $P = 0.01$]. Clinically relevant restenosis occurred in 56 of 257 homozygous carriers of the A-allele compared with 425 of 2811 heterozygous or homozygous carriers of the G-allele [21.8 vs. 15.1%, $P < 0.01$; OR 1.56 (95% CI 1.12–2.15), $P = 0.01$] (Figure 7F) also with a significant gene-dosage effect [GG 14.3 vs. AG 16.2 vs. AA 21.8%, $P < 0.01$]. Expectedly, restenosis occurred more often in patients treated with bare-metal stents (Supplementary material online, Table S5); there was, however, no significant interaction ($P = 0.93$) between genotype and stent type with respect to this outcome (Supplementary material online, Table S6).

Of note, the *TRPC6* locus does not harbour variants associated with coronary artery disease (CAD) (Supplementary material online, Figure S4) and the investigated variant rs2513192 did not show an association with CAD in the CARDIoGRAMplusC4D 1000 genome-wide association study³⁶ [OR 1.01 (95% CI 0.99–1.01), $P = 0.57$].

Discussion

Harmful vascular remodelling in patients after vascular interventions may lead to restenosis and, consequently, morbidity and mortality.⁴ In this study, we investigated the proteomic alterations secondary to

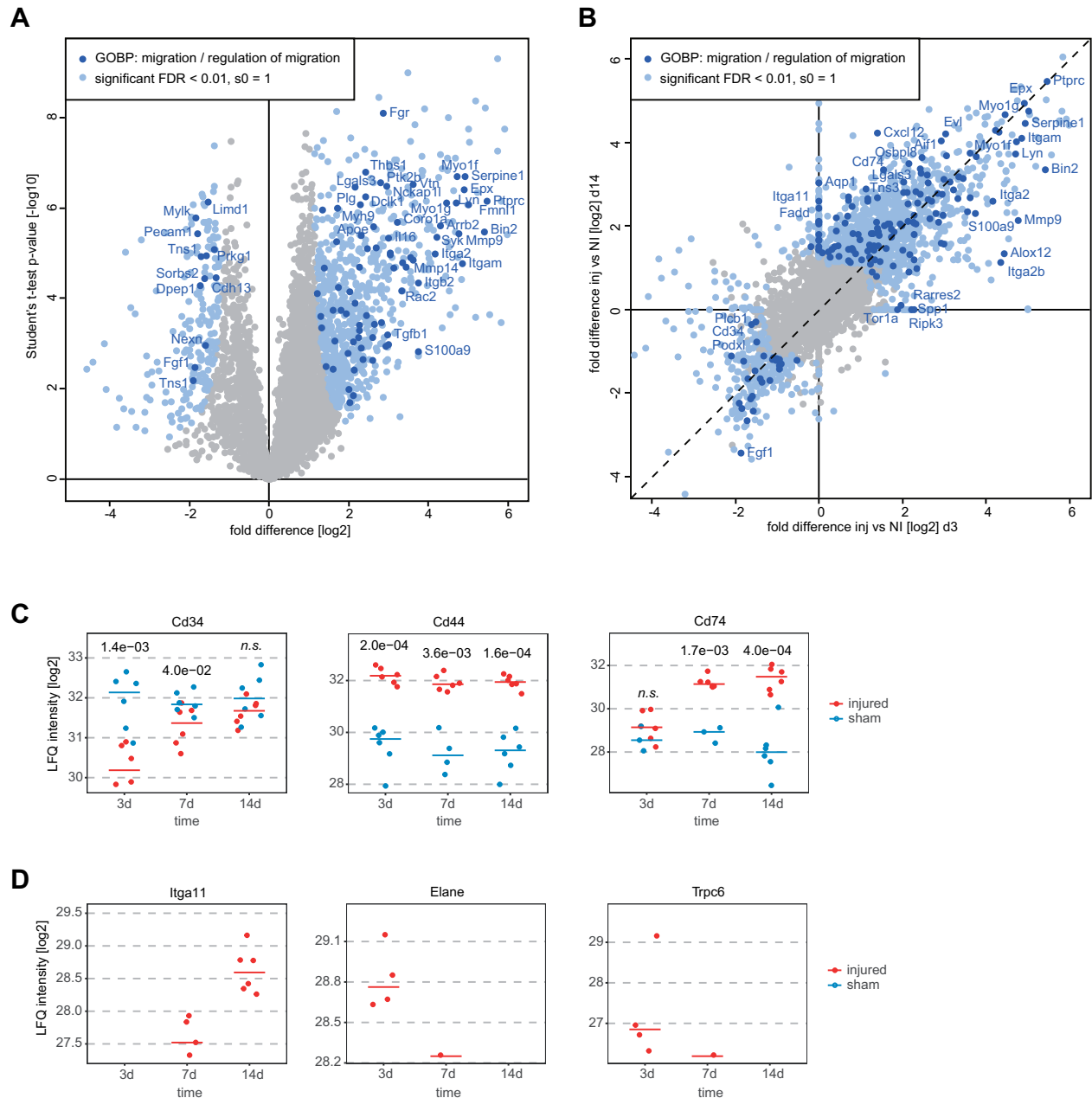


Figure 4 Regulation of proteins involved in cell migration during neointima formation. (A) Volcano plot with Student's *t*-test analysis as in Figure 2A with significantly regulated proteins annotated for the GOBP terms 'migration' or 'regulation of migration' marked in dark blue. (B) Correlation of average protein fold differences between injured and sham-treated femoral arteries at Day 3 vs. Day 14. Proteins significantly regulated at either Day 3 or Day 14 are marked in pale blue, proteins annotated for migration terms in dark blue as in (A). (C, D) Protein intensities of selected proteins involved in cell migration. Unpaired Student's *t*-test. Proteins depicted in (D) were exclusively detected under injury conditions. d, day(s); FDR, false discovery rate; GOBP, gene ontology biological process; inj, injured; LFI, label-free quantitation; NI, not injured.

vascular injury to provide a publicly accessible resource that helps to understand these pathophysiological processes at the proteomic level and to identify novel targets for their prevention.

Human vascular tissues cannot easily be sampled in general and especially not during the onset of neointima formation. In contrast, the

mouse is an ideal organism to study effects of vascular injury in a standardized manner. However, stent implantation and long-term observation of vascular remodelling are not yet feasible in mice. We were especially interested in early timepoints of neointima formation, as factors driving its onset may also serve as efficient clinical drug

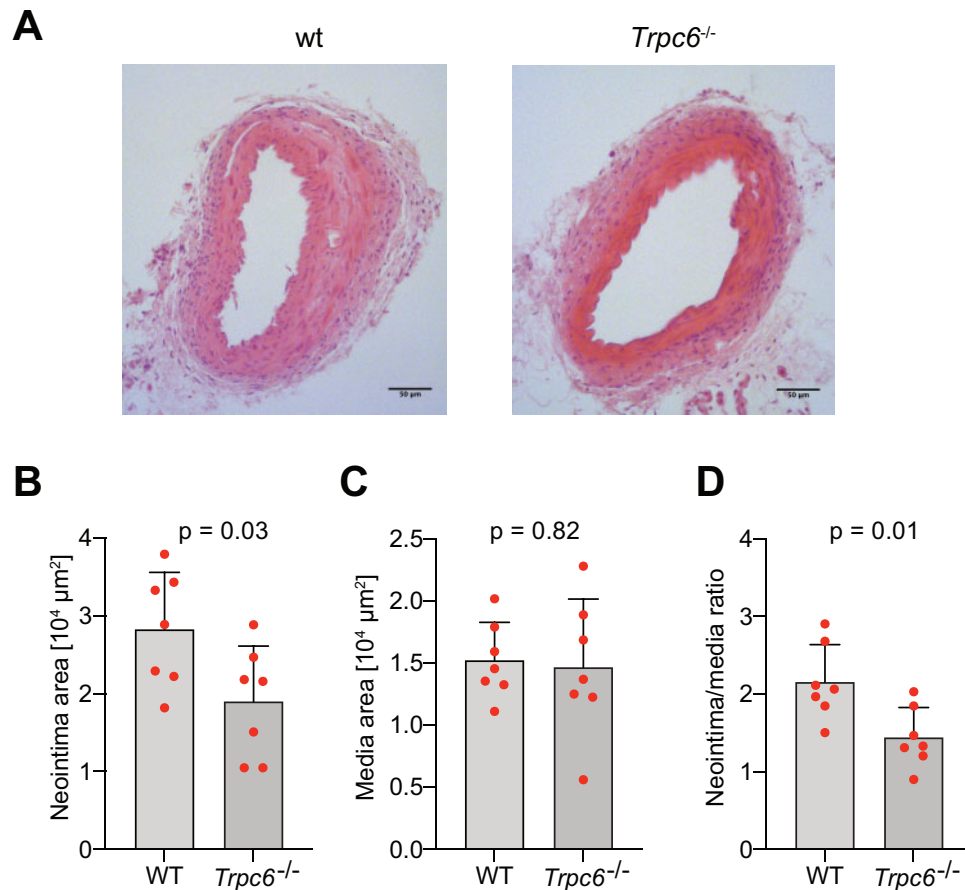


Figure 5 Neointima formation in *Trpc6*^{-/-} mice. (A) Haematoxylin and eosin stain of femoral arteries 28 days after wire-induced vascular injury. (B–D) Quantification of neointima area (B), media area (C), and neointima/media ratio (D) in *Trpc6*^{-/-} and wild-type mice 28 days after vascular injury ($n = 7$ each, unpaired *t*-test). Data are mean and SD. WT, wild-type.

targets. In single run, MS analyses of single femoral arteries, we detected almost 5000 proteins, representing the deepest proteomic investigation of vascular injury reported so far. Remarkably, more than half of these proteins were up- or down-regulated following vascular injury, indicating a drastic remodelling of this tissue.

The most prominent proteomic changes related to the ECM, cell migration, and immune response. Our time-resolved proteomic data allowed us to define proteins with early, late, or transient regulation in response to vascular injury. For example, while proteoglycan proteins of the coagulation pathway were specifically and transiently up-regulated at three days after injury, cartilage-related ECM proteins Col12a1 and Acan were specifically up-regulated at 14 days after injury. The unique up-regulation of Lamb1 compared with other laminin subunits proposes a new mechanistic role of this surface molecule in neointima formation, which remains to be explored. Laminin-1 has been reported to stimulate Mmp9 expression by activation of ERK signalling cascades in different cell types.^{37,38} However, as in our dataset, Lamb1 is up-regulated starting from Day 7, and Mmp9 is fully

up-regulated already at Day 3, a functional association via such mechanism appears unlikely.

From our resource of proteins with altered expression in vascular remodelling, we aimed at validating at least one molecular target to prevent restenosis. We selected *Trpc6* because the protein appeared likely to play a role in the initiation of neointima formation and because it was predominantly up-regulated at Day 3 after vascular injury. TRPC6 is a member of the family of classical or canonical transient receptor potential channels. It has six transmembrane domains and forms homotetramers or heterotetramers with other members of the TRPC subfamily,^{39–41} acting as plasmalemmal ion channels. It acts as a calcium-conducting, receptor-operated channel with an ion permeability ratio ($P_{Ca^{2+}}/P_{Na^{+}}$) of six.^{42–44} Following activation of phospholipase C by mechanical stress or agonists, the second messenger diacylglycerol is released and activates TRPC6-mediated calcium entry.⁴² A physiological relevance for TRPC6 has been described in neurons, tumours, immune, and blood cells as well as the kidney (reviewed in⁴⁵). In the heart, silencing of *TRPC6* was found to be anti-hypertrophic.⁴⁶ In vascular SMCs, TRPC6 is activated by α_1 -adrenoreceptors⁴⁷ and vasopressin,⁴⁸ while PDGF is

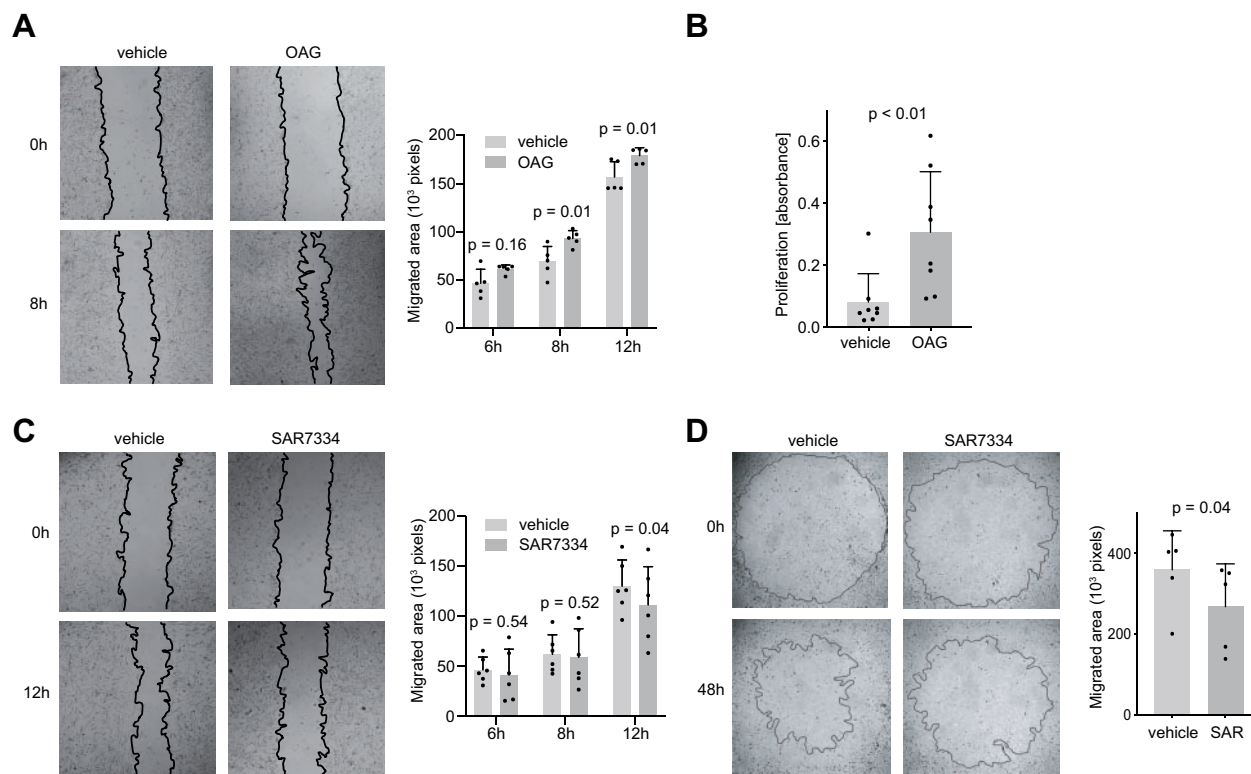


Figure 6 TRPC6 as a novel target in vascular remodelling. (A) *In vitro* scratch wound assay of human aortic smooth muscle cells after stimulation with 100 μ M OAG or vehicle, analysed after six, eight, and 12 h ($n = 5$ each, paired *t*-test). (B) Assessment of human aortic smooth muscle cell proliferation using BrdU enzyme-linked immunosorbent assay in the presence of 100 μ M OAG or vehicle ($n = 8$, paired *t*-test). (C) Scratch wound assay of human aortic smooth muscle cells after treatment with 100 nM SAR7334 or vehicle, analysed after six, eight, and 12 h ($n = 6$, paired *t*-test). (D) Radius migration assay of human aortic smooth muscle cell after coating with 100 nM SAR7335 or vehicle ($n = 5$, paired *t*-test). Data are mean and SD. h, hours; OAG, 1-oleoyl-2-acetyl-sn-glycerol; SAR, SAR7334.

associated with an up-regulation of *TRPC6* expression.⁴⁹ Interestingly, vasopressin has been shown to be up-regulated within hours after pressure overload of the heart.⁵⁰

Migration and proliferation of vascular SMCs are hallmarks of vascular remodelling including neointima formation. While we did not investigate effects on ECM remodelling secondary to modulating TRPC6 activity, we here found that the TRPC6 activator OAG leads to an increase of migration and proliferation. Therefore and in line with recent reports,⁵¹ increased TRPC6 protein levels might be a molecular correlate for initiation of SMC migration/proliferation and neointima formation. We further coated tissue culture dishes with the TRPC6 inhibitor SAR7334 and found that SMC migration was significantly reduced *in vitro*, proposing a clinical application of SAR7334 for coating stents (*Graphical abstract*). To investigate a role for TRPC6 in neointima formation, we compared *Trpc6*^{-/-} mice with wild-type mice at 28 days after vascular injury. *Trpc6*^{-/-} mice displayed reduced neointima formation, while the media area was not changed. These results are in line with reports that the inhibition of PDGF receptors reduces neointima formation⁵² and that calcium entry via TRPC channels might be involved in PDGF-mediated neointima formation.^{53,54} Of note, we cannot rule out any additional increased *Trpc6*

expression in other cell types, e.g. endothelial cells and fibroblasts, to be involved in the mechanism.

To extend our findings from mice to humans,^{55,56} we turned to genetic variants in humans. The *TRPC6* locus does not harbour a suggestive signal for CAD in recent genome-wide association studies.⁵⁷ However, we identified a common eSNP for *TRPC6* in tibial artery and strikingly, found a genotype that is associated with highest *TRPC6* mRNA levels and linked to increased PDGF-mediated proliferation capacity.

Finally, we asked if TRPC6 may have a role in restenosis secondary to coronary stenting. In a cohort including more than 4000 lesions in patients undergoing percutaneous coronary intervention followed by standardized assessment of restenosis, we found that genetically determined enhanced expression of *TRPC6* was associated with a higher risk of restenosis. While knowledge of the genotype associated with higher *TRPC6* expression may be useful in identifying patients at increased risk, the main implication of this genetic finding is—in addition to the mouse and *in vitro* data—that TRPC6 is a promising target in vascular injury and remodelling. Currently, inhibitors of the mechanistic target of rapamycin (mTOR) such as sirolimus, zotarolimus, or everolimus are used routinely as coatings of drug-eluting

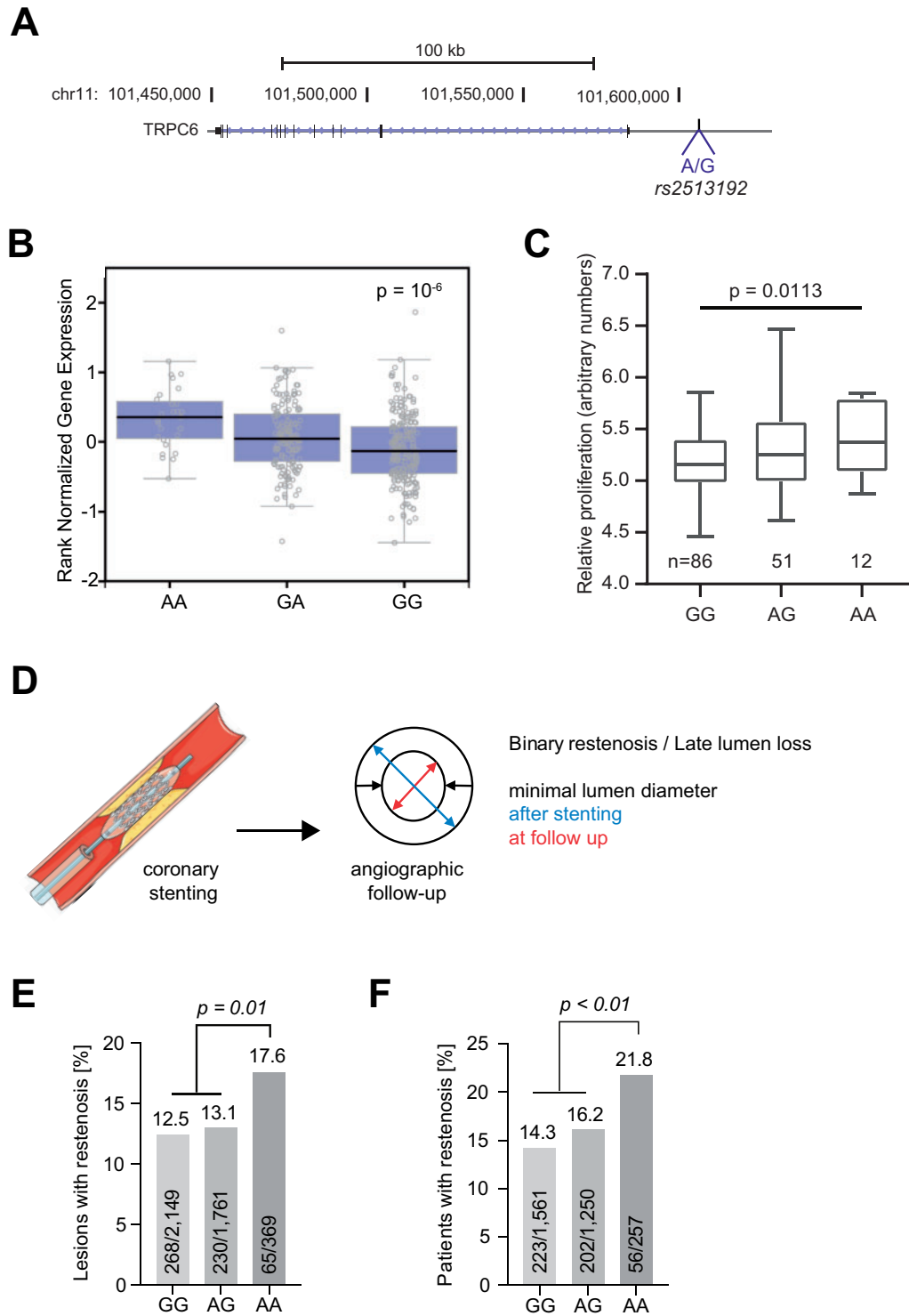


Figure 7 Effect of *TRPC6* genotype on smooth muscle cell migration and restenosis. (A) Location of rs2513192 at the *TRPC6* locus. (B) Association of the single nucleotide polymorphism rs2513192 with *TRPC6* expression (<https://gtexportal.org/home/>, accessed on 13 November 2018).³⁵ (C) Association of rs2513192 genotype with human aortic smooth muscle cell proliferation after stimulation with platelet-derived growth factor in $n = 149$ donors from the Systems Genetics Resource at the University of California, Los Angeles (<https://systems.genetics.ucla.edu/>). (D) Measurement of restenosis by angiographic follow-up. (E, F) Risk of restenosis after coronary stenting in homozygous AA lesions (E) and patients (F) compared with GG or AG lesions/patients (χ^2 test). Data are in per cent. chr, chromosome; kb, kilobases.

stents which has reduced the incidence of coronary restenosis compared with earlier used bare-metal stents.⁵⁸ These substances inhibit PDGF/PDGF receptor-mediated signalling via phosphoinositide 3-kinases.⁵⁹ Notably, PDGF-induced activation of TRPC6 via phospholipase C and diacylglycerol is independent of mTOR signalling. Inhibition of TRPC6 after coronary intervention might therefore be an alternative or complementary strategy to established mTOR inhibition and prevent restenosis.

In contrast to mTOR, TRPC6 is not essential for physiological functions of the body and is only activated under pathophysiological conditions such as focal segmental glomerulosclerosis, lung fibrosis, ischaemia, and reperfusion injury of heart and lung.⁴⁵ Inhibitors of TRPC6 should therefore be much safer than current mTOR inhibitors for prevention of neointima formation. TRPC6 inhibitors might be applied either systematically or as coating on drug-eluting stents. The role of TRPC6 in the initiation of neointima formation implied by our data suggests that TRPC6 inhibition would mostly be beneficial in the early phase after interventional treatment of blocked arteries.

Supplementary material

Supplementary material is available at *European Heart Journal* online.

Acknowledgements

We would like to thank Dirk Wischnewski, Korbinian Mayr, and Igor Paron for excellent technical assistance as well as Tan An Dang and Carina Mauersberger for assistance with animal experiments.

Funding

This work has been funded by the Deutsche Forschungsgemeinschaft (DFG) as part of the Sonderforschungsbereich CRC 1123 (B02 to H.S. and T.K.; B03 to M.D.), the Transregio TRR 152 (project 1 to V.F.; project 16 to A.D.), and the Corona Foundation (Junior Research Group *Translational Cardiovascular Genomics*, to T.K.). This study was also supported by grants from the Fondation Leducq (CADgenomics: Understanding CAD Genes, 12CVD02, and PlaQomics to H.S.), the German Federal Ministry of Education and Research (BMBF) within the framework of the e: Med research and funding concept (e: AtheroSystMed, grant 01ZX1313A-2014 to H.S. and M.M.), and the European Union

Seventh Framework Programme FP7/2007-2013 under grant agreement n° HEALTH-F2-2013-601456 (CVgenes-at-target to H.S.).

Conflict of interest: The authors' institutions filed a patent application (H.S., A.K., and T.K. are named inventors) on the use of TRPC6 inhibitors for prevention of restenosis after angioplasty and stent implantation. H.S. has received personal fees from MSD SHARP and DOHME, AMGEN, Bayer Vital GmbH, Boehringer Ingelheim, Daiichi-Sankyo, Novartis, Servier, Brahms, Bristol-Myers-Squibb, Medtronic, Sanofi Aventis, Synlab, Pfizer, and Vifor T as well as grants and personal fees from Astra-Zeneca outside the submitted work. The other authors report no conflict of interest.

Data availability

All data are presented in the main manuscript and the [Supplementary material online](#).

References

1. Timmis A, Townsend N, Gale CP, Torbica A, Lettino M, Petersen SE, Mossialos EA, Maggioni AP, Kazakiewicz D, May HT, De Smedt D, Flather M, Zuhke L, Beltrame JF, Huculeci R, Tavazzi L, Hindricks G, Bax J, Casadei B, Achenbach S, Wright L, Vardas P; European Society of Cardiology. European Society of Cardiology: cardiovascular disease statistics 2019. *Eur Heart J* 2020;**41**:12–85.
2. Leong DP, Joseph PG, McKee M, Anand S, Teo KK, Schwalm J-D, Yusuf S. Reducing the global burden of cardiovascular disease, part 2: prevention and treatment of cardiovascular disease. *Circ Res* 2017;**121**:695–710.
3. Kastrati A, Mehilli J, Dirschinger J, Pache J, Ulm K, Schühlen H, Seyfarth M, Schmitt C, Blasini R, Neumann FJ, Schomig A. Restenosis after coronary placement of various stent types. *Am J Cardiol* 2001;**87**:34–39.
4. Cassese S, Byrne RA, Schulz S, Hoppman P, Kreutzer J, Feuchtenberger A, Ibrahim T, Ott I, Fusaro M, Schunkert H, Laugwitz K-L, Kastrati A. Prognostic role of restenosis in 10 004 patients undergoing routine control angiography after coronary stenting. *Eur Heart J* 2015;**36**:94–99.
5. Mayr M, Chung Y-L, Mayr U, Yin X, Ly L, Troy H, Fredericks S, Hu Y, Griffiths JR, Xu Q. Proteomic and metabolomic analyses of atherosclerotic vessels from apolipoprotein E-deficient mice reveal alterations in inflammation, oxidative stress, and energy metabolism. *Arterioscler Thromb Vasc Biol* 2005;**25**:2135–2142.
6. Bagnato C, Thumar J, Mayya V, Hwang S-I, Zebroski H, Claffey KP, Haudenschild C, Eng JK, Lundgren DH, Han DK. Proteomics analysis of human coronary atherosclerotic plaque: a feasibility study of direct tissue proteomics by liquid chromatography and tandem mass spectrometry. *Mol Cell Proteomics* 2007;**6**:1088–1102.
7. Hao P, Ren Y, Pasterkamp G, Moll FL, de Kleijn DPV, Sze SK. Deep proteomic profiling of human carotid atherosclerotic plaques using multidimensional LC-MS/MS. *Proteomics Clin Appl* 2014;**8**:631–635.

References 8–59 are available in the [Supplementary material online](#).